

RESEARCH PAPER

Compact dual-band antennas with large frequency ratio and bandwidth enhancement for wireless applications

ABDELHEQ BOUKARKAR, XIAN QI LIN AND YUAN JIANG

In this paper, compact single-feed dual-band antennas for different wireless applications are proposed. First, a dual-band antenna with a comparatively large frequency ratio of 2.58 is designed. Then, a novel dual-band antenna is introduced in order to enhance the upper frequency band. The technique consists of modifying the feed line structure, which leads to a 9.23% of impedance bandwidth at the central frequency of 6.5 GHz instead of 2.06%. The designed antennas are fabricated and tested in the laboratory and in a small anechoic chamber in order to measure their reflection coefficient, gains, and efficiencies. Good agreement between simulated and measured results is obtained. The designed antennas are particular because they have low profile, very simple single-feed technique, can be designed for large frequency ratios, and also the bandwidth can be clearly enhanced. Therefore, they can be used for different wireless applications.

Keywords: Antennas and propagation for wireless systems, Antenna design, Modeling and measurements

Received 15 June 2016; Revised 20 September 2016; Accepted 23 September 2016; first published online 21 December 2016

I. INTRODUCTION

In recent years, compact size dual-band antennas with simple structures are extremely needed for different wireless communication applications. Several designs for dual-band antennas have been introduced and studied [1–13]. In [1], an analysis and design of a compact dual-band directional antenna for 2.4/5-GHz wireless access point and RFID reader application is proposed. The antenna realizes a high gain however it occupies a large space of $43 \times 26 \times 12 \text{ mm}^3$ with a large ground plane of $100 \times 60 \text{ mm}^2$. In [2], a novel dual-band antenna for wireless communication applications is fabricated. The antenna is fed by a coaxial probe, which increases its size and increases also the complexity level of its fabrication comparing with coplanar waveguide (CPW) feed technique adopted in our designs. In [3], a compact dual-band antenna for wireless body-area network applications is fabricated. The antenna suffers from narrow bandwidths of only 1.2 and 2.0% at the lower and upper bands, respectively. Tunable dual-band antennas for 0.7–1.1-GHz and 1.7–2.3-GHz carrier aggregation systems are presented in [4]. The antennas solve the drawback of narrow bandwidths by using varactor diodes. However, the efficiencies are found to be poor mainly due to the RF power dissipated by the varactors. On the other hand, designing dual-band antennas with large frequency ratios, which operate in different frequency

bands may be required for some applications such as satellite communications [5] and ISM bands [6]. In this paper, we will introduce the design of two dual-band antennas based on the mechanism of magnetic dipoles obtained by shorting one edge of the radiating patches to the ground plane [7]. The first designed antenna has a large frequency ratio of 2.58 compared with that one obtained in [8–11]. In order to enhance the impedance bandwidth of the upper band, a dual-band antenna is designed based on the modification of the RF feed line structure. The technique avoids the use of lumped components, which leads to an acceptable maximum measured gain of 6.1 dBi with a maximum measured efficiency of 74%. A measured bandwidth value of 9.23% is obtained at the central frequency 6.5 GHz, which is much higher compared with the values obtained in [3, 4], and [8–10]. We note that the designed antennas are fed using a single short-ended CPW feed line. The following sections are dedicated to the design of the two antennas including all the simulation and measurement results.

II. DESIGN OF COMPACT DUAL-BAND ANTENNA WITH LARGE FREQUENCY RATIO

A) Antenna structure and design principles

All the designs of this paper are printed on the substrate F4B having a thickness of $h = 1.964 \text{ mm}$, a relative permittivity of 2.55, and a loss tangent of 0.002. Figure 1 shows the structure of the single-feed dual-band antenna with large frequency ratio.

School of Electronic Engineering, University of Electronic Science and Technology of China, Chengdu 611731, China

Corresponding author:

X.Q. Lin

Email: xqlin@uestc.edu.cn

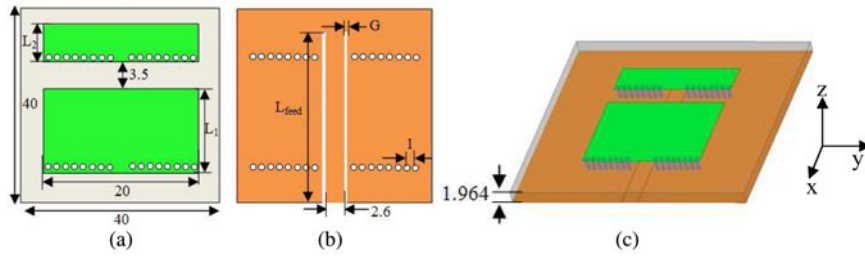


Fig. 1. Structure of the compact dual-band antenna with large frequency ratio (unit: mm); $L_1 = 15.5$, $L_2 = 5.4$, $G = 0.1$, $L_{feed} = 35.5$. (a) Top view, (b) bottom view, (c) perspective view.

The top layer of the antenna contains two metallic patches shorted to the ground plane on one edge using metalized vias. The metalized vias have a diameter of 0.6 mm with a spacing of 1 mm between them. They act like a shorting wall, which reduces the length of the radiating patches to approximately a quarter wavelength instead of a half wavelength corresponding to an ordinary patch antenna without shoring edges. The width of the patches is arbitrarily chosen. In fact, it is found that the bigger the patch width the higher the antenna gain. The main criterion for our designs consists of setting the length of the patches L_1 , and L_2 equal to a quarter wavelength. For this first antenna prototype, both patches have a width $W = 20$ mm and their lengths L_1 , L_2 are set equal to a quarter wavelength according to the desired operating frequencies. As depicted in Fig. 2, at the resonant frequencies, the current flows from the top radiating patches to the ground plane through the metalized vias creating an open loop, which can be regarded as a magnetic dipole antenna [7, 14].

A single short-ended CPW line is used for the radio frequency (RF) feeding of the two bands. A good impedance value of $50\text{-}\Omega$ is obtained by controlling the values of its length L_{feed} and the gap G . As we shorted the radiating patches on one edge to the ground plane, the even resonant modes are suppressed so a large frequency ratio can be obtained [15]. We note that the disposition of the two patches is chosen in order to make simple the RF feeding structure. Indeed, the two patches are fed in series, which leads to a simple control of the impedance match by simply adjusting the length L_{feed} . The designed antenna can also realize small frequency ratios as shown in the following parametric study.

B) Parametric study

The software used for the simulation is high frequency structure simulator based on finite elements method. The aim of this parametric study is to demonstrate that our dual-band antenna can be designed for large and small frequency ratios. We keep unchanged all the antenna parameters while we sweep the patch length L_2 . Figure 3 illustrates the corresponding simulation results for the reflection coefficient $|S_{11}|$. The upper frequency band is changed according to the length L_2 , which corresponds to a quarter wavelength. We note that the lower frequency band is not affected by changing the length L_2 . This result demonstrates that the frequency ratio can be tuned according to the desired operating frequencies. After running a parametric study, an antenna prototype is fabricated in order to validate the simulation results.

C) Simulation and measurement results

An Agilent N5244A laboratory network analyzer is used to measure the antenna reflection coefficient $|S_{11}|$. Different antenna gains as well as radiation patterns are obtained in an anechoic chamber. Figure 4 illustrates the simulated and measured $|S_{11}|$ of the antenna.

The first measured operating frequency $f_1 = 2.99$ GHz corresponding to the lower band is nearly equal to the simulated value 2.94 GHz. The second measured operating frequency occurs at $f_2 = 7.7$ GHz with a good impedance match and 400 MHz of bandwidth evaluated at -10 dB. Above 6 GHz, the relative permittivity of the substrate used in this design (F4B) is less stable; this is why there is a frequency shifting between the simulated and measured values of f_2 . A comparatively high frequency ratio $f_2/f_1 = 2.58$ is

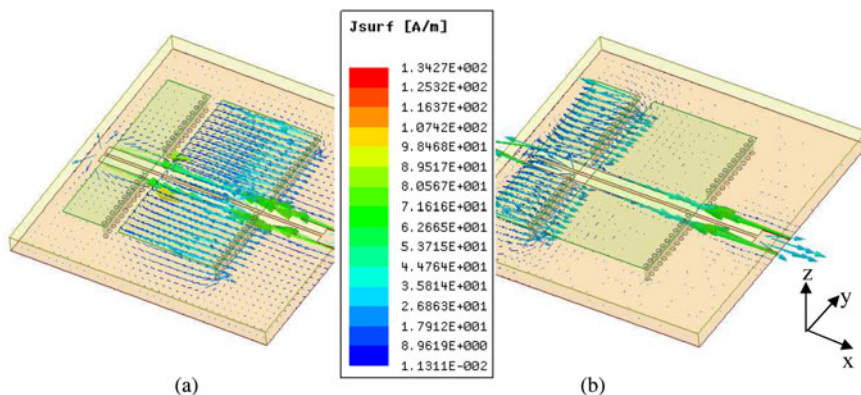


Fig. 2. Current distribution at the resonant frequencies of the antenna. (a) At 2.94 GHz, (b) at 7.5 GHz.

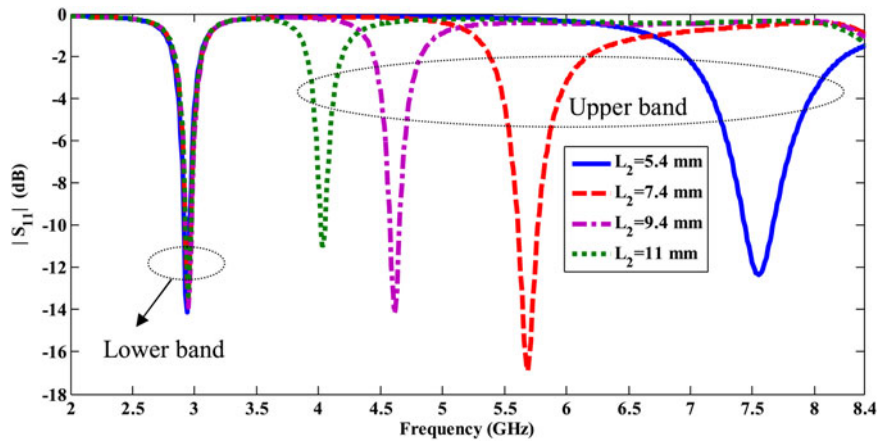


Fig. 3. The simulated reflection coefficient $|S_{11}|$ when L_2 is tuned.

realized by this antenna. Figure 5 shows a sample of simulated and measured radiation patterns at f_1 and f_2 . The maximum level of cross polarization obtained in E -plane is -18 dBi for both resonant frequencies. In H -plane, the level of cross polarization in the direction of maximum radiation is less than -22 dBi. The measured peak gains and efficiencies at f_1 and f_2 are respectively, 2.97 dBi-61% and 5.7 dBi-73%.

A comparative study of our work with some references is given in Table 1. Note that the lower resonant frequency is considered for computing the guided wavelength λ_g in the following table. According to Table 1 and compared with our design, the antenna presented in [8] has a large electrical size and a small frequency ratio of only 1.14. The design introduced in [9] has a low gain value at the lower band and uses two PIN diodes to select only one operating frequency at one time. Although the antenna realizes 2.01 of frequency ratio, the use of PIN diodes will increase the complexity of the design once a DC bias circuit is introduced as well as decreasing the antenna efficiency. The antenna presented in [10] has a very high thickness and uses a complex feeding system for the dual-band operation. We conclude that the designed antenna presents a large frequency ratio, an acceptable peak gain, and a compact size with simple RF feeding structure, which makes it a good candidate for wireless applications. In the following

section, another dual-band antenna with improvement of the upper frequency bandwidth is further discussed.

III. DESIGN OF COMPACT DUAL-BAND ANTENNA WITH BANDWIDTH ENHANCEMENT

A) Antenna structure and design principles

After designing a single-feed dual-band antenna with a large frequency ratio, the next step is to design another dual-band with improvement of the upper frequency bandwidth. The technique consists of modifying the RF feed line structure in order to create another resonant frequency. The antenna structure is given in Fig. 6.

The radiating patches on the top side of the antenna have a width $W = 26$ mm. The lengths of the patches are chosen to excite two operating frequencies 2.84 and 6.19 GHz. The geometrical dimensions of the feed line denoted by W_g and L_g are adjusted carefully to get the desired resonant frequency in the upper band. By combining the resonant frequency obtained through the radiating patch L_2 and the one created by modifying the RF feed line structure, we get a wide upper

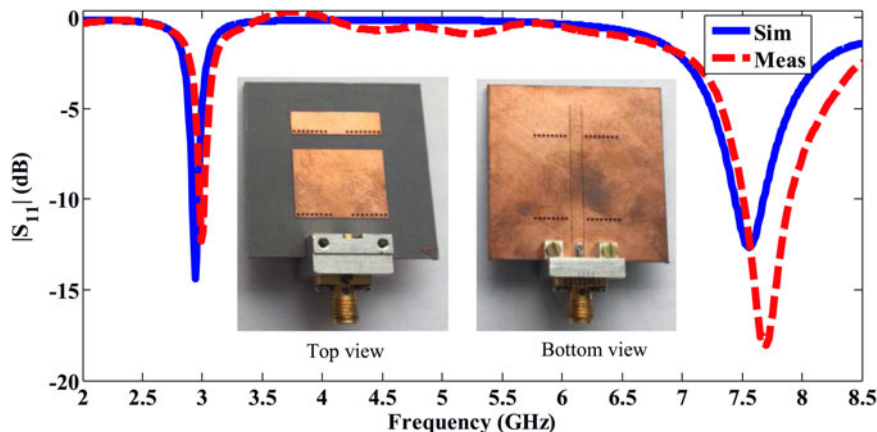


Fig. 4. Simulated and measured $|S_{11}|$ of the dual-band with large frequency ratio.

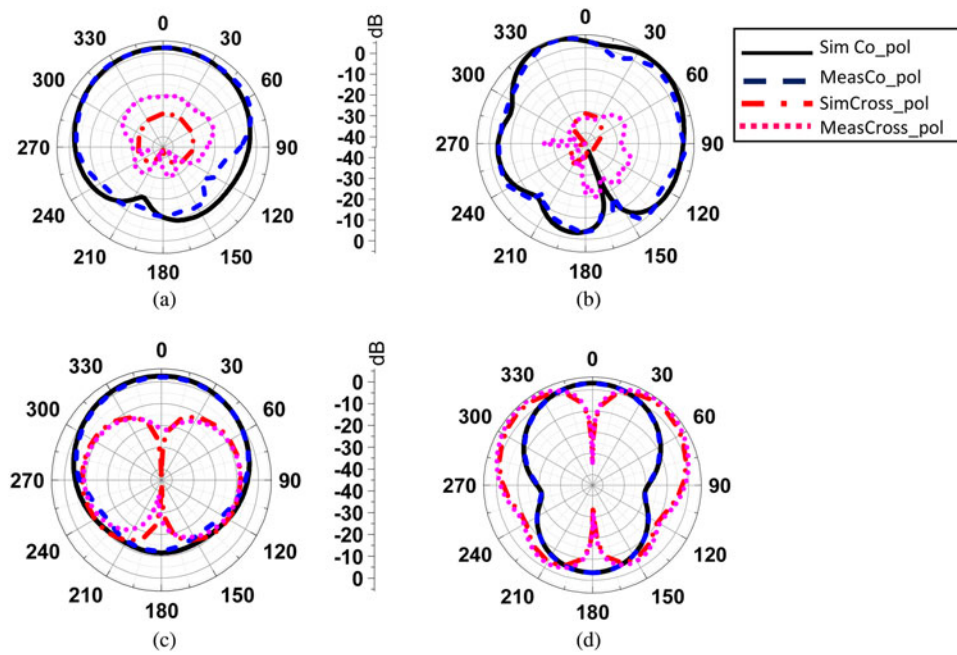


Fig. 5. Simulated and measured radiation patterns. (a) $f_1 = 2.99$ GHz in E -plane ($\varphi = 0^\circ$), (b) $f_2 = 7.7$ GHz in E -plane ($\varphi = 0^\circ$), (c) $f_1 = 2.99$ GHz in H -plane ($\varphi = 90^\circ$), (d) $f_2 = 7.7$ GHz in H -plane ($\varphi = 90^\circ$).

bandwidth. A parametric study showing the effects of W_g and L_g on the resonant frequency of the upper band is carried out. We note that the impedance match is controlled by adjusting the dimensions of the feed line. The antenna overall size is $40 \times 40 \times 1.964$ mm³.

Table 1. Comparison between our work and some references.

References	[8]	[9]	[10]	Our work
Antenna thickness (mm)	0.203	0.875	23.14	1.964
Radiating patches electrical size	$0.38\lambda_g \times 0.40\lambda_g$	$0.21\lambda_g \times 0.37\lambda_g$	$4\lambda_g \times 4\lambda_g$	$0.32\lambda_g \times 0.38\lambda_g$
f_1 (GHz)	12.5	3.54	6.9	2.99
f_2 (GHz)	14.25	7.12	13.3	7.7
Frequency ratio	1.14	2.01	1.93	2.58
Gain lower band (dBi)	4.4	0.35	16.5	2.97
Gain upper band (dBi)	5.6	7.87	20.9	5.7

B) Parametric study

This parametric study aims to investigate the influence of the feed line geometrical parameters denoted by W_g and L_g on the antenna resonant frequencies. First, all the antenna parameters are kept unchanged and only W_g is changed.

According to Fig. 7, when the feed line is not modified (kept the same as the structure shown in Fig. 1) with $W_g = 2.6$ mm, the antenna presents an upper impedance bandwidth of only 130 MHz (2.06%) evaluated at -10 dB of $|S_{11}|$ and centered at 6.3 GHz. By decreasing the value of W_g , another resonant frequency appears just near the operating frequency excited by the patch L_2 . The largest bandwidth is obtained when $W_g = 0.4$ mm. Then, the length L_g is adjusted for a good impedance matching as shown in Fig. 8.

In fact to realize a wide upper bandwidth, two resonant frequencies are carefully adjusted and combined together. The first resonant frequency is controlled and excited by the patch L_2 while the second resonant frequency is excited by the feeding line, which creates an additional resonant mode.

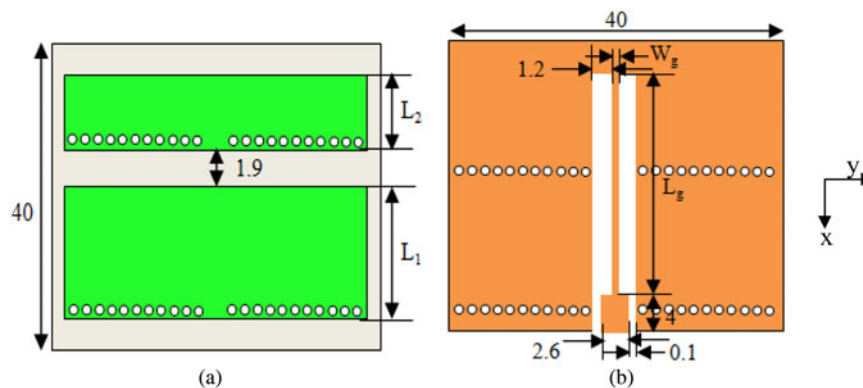


Fig. 6. Structure of the compact dual-band with bandwidth enhancement (unit: mm); $L_1 = 15.6$, $L_2 = 6.7$, $L_g = 34.1$, $W_g = 0.4$. (a) Top view, (b) bottom view.

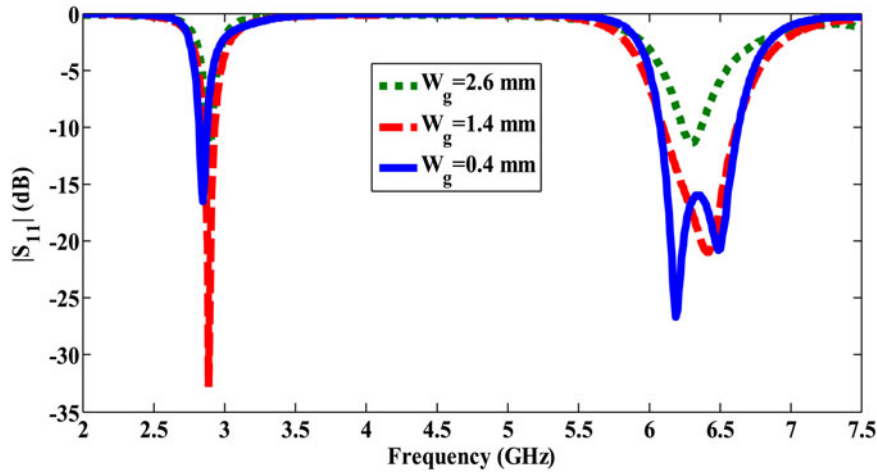


Fig. 7. The simulated reflection coefficient $|S_{11}|$ when W_g is tuned.

By combining two resonant modes, one created by the patch L_2 and the second one created by the feeding line, a wide bandwidth with better impedance match can be obtained. To demonstrate that there are two resonant frequencies in the upper band, the input impedance Z_{11} is displayed. The

second resonant frequency can be controlled and adjusted by tuning the value of W_g . According to Fig. 9, two resonant frequencies are presented, the first one occurs at 6.2 GHz corresponding to the patch L_2 ; It remains unchanged when W_g is tuned. The second resonant frequency increases by increasing

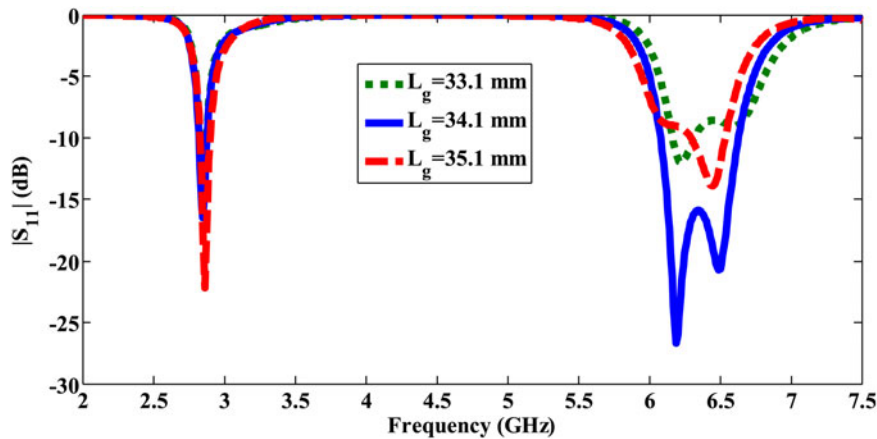


Fig. 8. The simulated reflection coefficient $|S_{11}|$ when L_g is tuned.

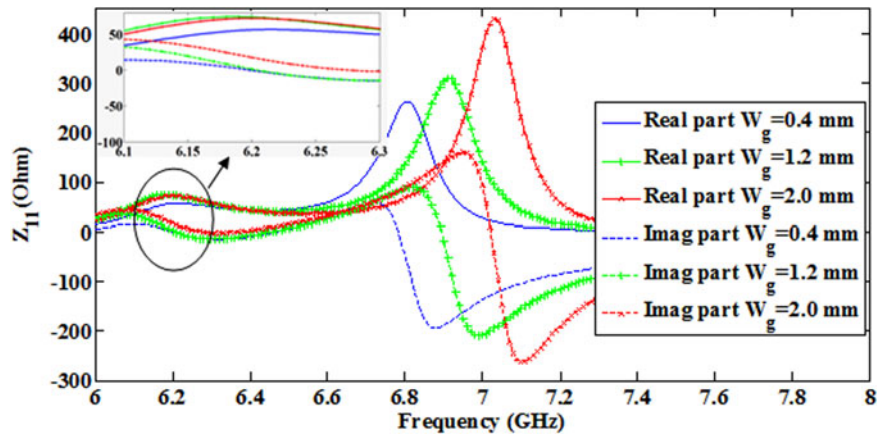


Fig. 9. The simulated input impedance when W_g is tuned.

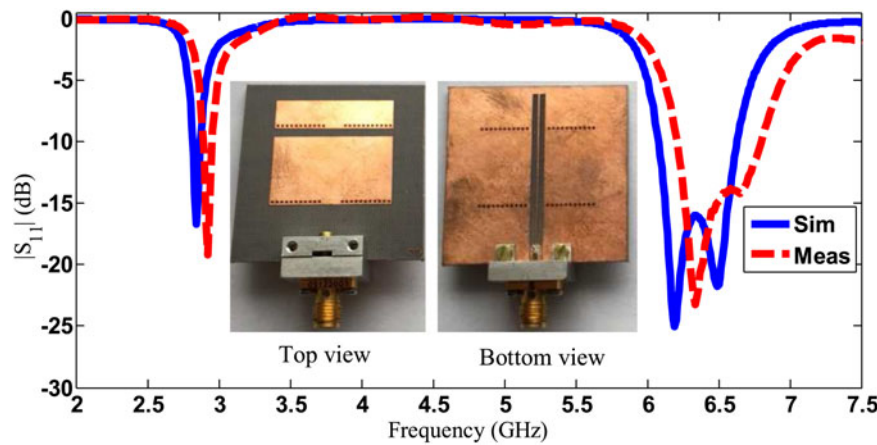


Fig. 10. Simulated and measured $|S_{11}|$ of the dual-band with bandwidth enhancement.

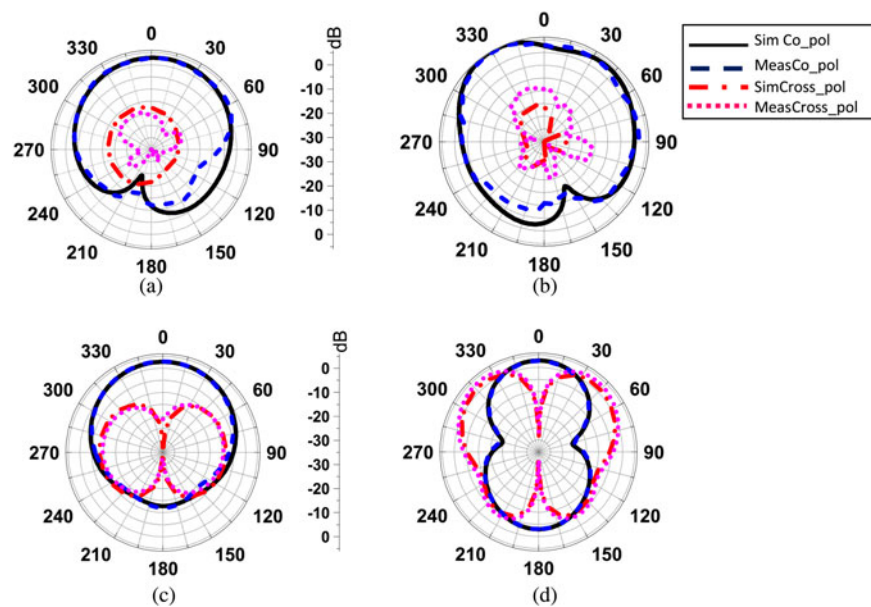


Fig. 11. Simulated and measured radiation patterns. (a) $f_1 = 2.93$ GHz in E -plane ($\varphi = 0^\circ$), (b) $f_2 = 6.5$ GHz in E -plane ($\varphi = 0^\circ$), (c) $f_1 = 2.93$ GHz in H -plane ($\varphi = 90^\circ$), (d) $f_2 = 6.5$ GHz in H -plane ($\varphi = 90^\circ$).

Table 2. Comparison between our work and other papers.

References	[3]	[8]	[9]	Our work
RF feeding technique	Coaxial probe	Microstrip line	Microstrip line	CPW feed line
Radiating patches electrical size	$0.39\lambda_g \times 0.39\lambda_g$	$0.38\lambda_g \times 0.40\lambda_g$	$0.21\lambda_g \times 0.37\lambda_g$	$0.37\lambda_g \times 0.40\lambda_g$
Center freq lower band (GHz)	2.44	12.5	3.54	2.93
Bandwidth (%)	1.2	5.5	1.4	1.9
Center freq upper band (GHz)	5.78	14.25	7.12	6.5
Bandwidth (%)	2	3.5	1.6	9.23
Gain lower band (dBi)	2.13	4.4	0.35	2.95
Gain upper band (dBi)	5.16	5.6	7.87	6.1

the width W_g . We note also from Fig. 9 that by reducing the line width W_g the two resonant frequencies get closer and can be combined to realize a wide frequency bandwidth.

C) Simulation and measurement results

An antenna prototype is fabricated to validate the proposed approach. The simulated and measured reflection coefficient

$|S_{11}|$ of the antenna as well as the radiation patterns are carried out. Figure 10 shows the simulated and measured $|S_{11}|$. The measured result of the $|S_{11}|$ reveals two frequency bands, the lower band is centered at 2.93 GHz and the upper band ranges from 6.2 to 6.8 GHz (9.23% at the central frequency 6.5 GHz) evaluated at -10 dB. An important bandwidth enhancement from 2.06 to 9.23% is obtained by modifying the feed line structure of this antenna. Some

samples of simulated and measured radiation patterns are shown in Fig. 11. The minimum measured peak gain is 2.95 dBi for the operating frequency 2.93 GHz and goes from 5.3 to 6.1 dBi for the band 6.2–6.8 GHz. The antenna measured efficiencies take values in the interval [61, 74%].

To demonstrate the importance of this design, a comparative study with other references is displayed in Table 2. According to Table 2 and compared with [3], our design uses a simple CPW RF feeding line, which reduces the fabrication complexity. Also the bandwidths for the lower and upper frequency bands are much higher than the values realized by the design of [3]. In [8], the antenna realizes a value of 5.5% of bandwidth at the lower band. However, the RF microstrip feed line have to be properly located; otherwise the antenna will resonate only at a single frequency. In our design, the RF feeding line is very easy to adjust by a simple control of its length and width. In [9], beside the low values of the bandwidths, the antenna gain is found to be very poor at the lower frequency band compared with the value obtained in our design. We deduce that our antenna has better performance including compact size and wide upper impedance bandwidth with a very simple CPW RF feed line.

IV. CONCLUSION

In this paper, two antennas are presented and discussed. The first one is a single-feed dual-band antenna having a large frequency ratio of 2.58. The second antenna has the particularity of realizing a comparatively wide impedance bandwidth of 9.23% at the central frequency 6.5 GHz. A simple RF single-feed technique leading to ease of fabrication and compact size is adopted. The two designs have an acceptable measured gains and efficiencies with low profile. Therefore, they can find their use in wireless communication applications.

ACKNOWLEDGEMENTS

This work was supported in part by NSFC (No. 61571084), in part by NCET (No. NCET-13-0095), in part by the FRF for CU (No. ZYGX2014J016), and in part by the SRF for ROCS, SEM.

REFERENCES

- [1] Quan, X.; Li, R.; Cui, Y.; Tentzeris, M.: Analysis and design of a compact dual-band directional antenna. *IEEE Antennas Wireless Propag. Lett.*, **11** (2012), 547–550.
- [2] Zhu, X.Q.; Guo, Y.X.; Wu, W.: A novel dual-band antenna for wireless communication applications. *IEEE Antennas Wireless Propag. Lett.*, **15** (2016), 516–519.
- [3] Zhu, X.Q.; Guo, Y.X.; Wu, W.: A compact dual-band antenna for wireless body-area network applications. *IEEE Antennas Wireless Propag. Lett.*, **15** (2016), 98–101.
- [4] Avser, B.; Rebeiz, G.M.: Tunable dual-band antennas for 0.7–1.1-GHz and 1.7–2.3-GHz carrier aggregation systems. *IEEE Trans. Antennas Propag.*, **63** (2015), 1498–1504.
- [5] Smith, T.; Gothelf, U.; Kim, O.S.; Breinbjerg, O.: An FSS-backed 20/30 GHz circularly polarized reflectarray for a shared aperture L and

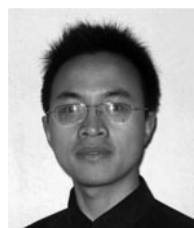
Ka-band satellite communication antenna. *IEEE Trans. Antennas Propag.*, **62** (2014), 661–668.

- [6] Feng, L.Y.; Leung, K.W.: Dual-frequency folded-parallel-plate antenna with large frequency ratio. *IEEE Trans. Antennas Propag.*, **64** (2016), 340–345.
- [7] He, K.; Gong, S.X.; Gao, F.: A wideband dual-band magneto-electric dipole antenna with improved feeding structure. *IEEE Antennas Wireless Propag. Lett.*, **13** (2014), 1729–1732.
- [8] Chen, C.H.; Wang, X.L.; Wu, W.: Compact single-feed dual-frequency dual-polarization microstrip antenna. *Electron. Lett.*, **46** (2010), 1362–1363.
- [9] Meng, F.; Sharma, S.K.: Single feed dual-frequency orthogonal linear-polarization microstrip patch antenna with large frequency ratio, in *Int. Symp. on Antennas and Propagation & USNC/URSI National Radio Science Meeting*, Vancouver, 2015, 836–837.
- [10] Meng, F.; Sharma, S.K.: A dual-band high-gain resonant cavity antenna with a single layer superstrate. *IEEE Trans. Antennas Propag.*, **63** (2015), 2320–2325.
- [11] Li, X.; Yang, S.; Nie, Z.: A novel dual-band patch antenna with high frequency band ratio. *Cross Strait Quad-Regional Radio Science and Wireless Technology Conf. (CSQRWC)*, Chengdu, 2013, 269–272.
- [12] Liu, S.; Wu, W.; Fang, D.G.: Single-feed dual-layer dual-band E-shaped and U-slot patch antenna for wireless communication application. *IEEE Antennas Wireless Propag. Lett.*, **15** (2016), 468–471.
- [13] Quan, X.; Li, R.; Jin, G.; Tentzeris, M.M.: Development of a directional dual-band planar antenna for wireless applications. *IET Microw. Antennas Propag.*, **7** (2013), 245–250.
- [14] Li, M.; Lin, X.Q.; Chin, J.Y.; Liu, R.; Cui, T.J.: A novel miniaturized printed planar antenna using split-ring resonator. *IEEE Antennas Wireless Propag. Lett.*, **7** (2008), 629–631.
- [15] Cabedo-Fabres, M.; Antonino-Daviu, E.; Valero-Nogueira, A.; Bataller, M.F.: The theory of characteristic modes revisited: a contribution to the design of antennas for modern applications. *IEEE Antennas Propag. Mag.*, **49** (2007), 52–68.



Abdelheq Boukarkar was born in Algeria on November 11, 1984. He received the B.S. degree in 2009 and the M.S. degree in 2015 from the University of Electronic Science and Technology of China (UESTC) and he is working toward the Ph.D. degree in Electronic Engineering. His research interests include antenna design and reconfigurable

RF/Microwave circuits.



Xian Qi Lin was born in Zhejiang Province, China, on July 9, 1980. He received the B.S. degree in Electronic Engineering from UESTC (University of Electronic Science and Technology of China), in 2003, and Ph.D. degree in Electromagnetic and Microwave Technology from Southeast University, Nanjing, China, in 2008. He joined the Department of

Microwave Engineering at UESTC in August 2008, and has become an Associate Professor and a doctoral supervisor since July 2009 and December 2011, respectively. From September 2011 to September 2012, he was a post-doc researcher in the Department of Electromagnetic Engineering at Royal

Institute of Technology (KTH), Sweden. He has authored over 10 patents, over 40 scientific journal papers, and has presented over 20 conference papers. His research interests include microwave/millimeterwave circuits, and antennas. Dr. Lin is a member of IEEE and a reviewer of many well-known journals such as IEEE- MTT/AP/MWCL/AWPL, JEMWA/PIER and EL.



Yuan Jiang was born in Jiangsu China. He received the B.S. degree in 2006 and is working toward the Ph.D. degree in Electronic Engineering from the University of Electronic Science and Technology of China (UESTC). His research interests include reconfigurable RF/Microwave circuits and antennas.